RSC Advances

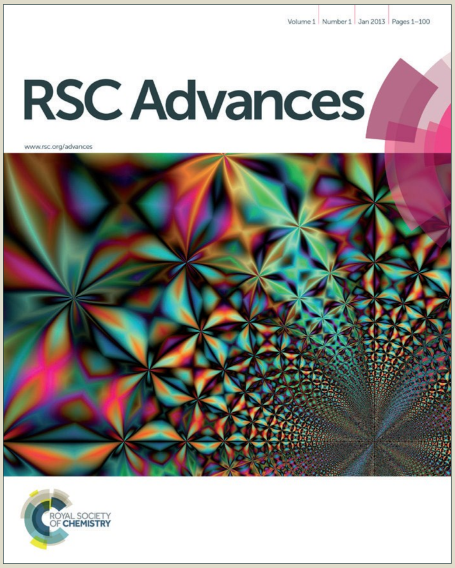

ROYAL SOCIETY OF CHEMISTRY

www.rsc.org/advances

Journal Name

ARTICLE

Received 00th January 20xx,
Accepted 00th January 20xx

DOI: 10.1039/x0xx00000x

www.rsc.org/

Tuning the Physical Properties of Pyrrolo[3,4-c]pyrrole-1,3-dione-Based Highly Efficient Large Band Gap Polymer via the Chemical Modification on the Polymer Backbone for Polymer Solar Cells

Vellaiappillai Tamilavan,[a] Dal Yong Lee,[b] Rajalingam Agneeswari,[a] Shinuk Cho,[c] Youngeup Jin,[d] Sung Heum Park,*[b] and Myung Ho Hyun*[a]

A systematic modulation of the photo-physical properties of high energy converting large band gap (2.04 eV) alternating polymer (PBDTT-DPPD) containing electron rich 2D-conjugated benzodithiophene (BDTT) and weak electron accepting pyrrolo[3,4-c]pyrrole-1,3-dione (DPPD) derivatives via the incorporation of a relatively strong electron accepting thieno[3,4-c]pyrrole-4,6-dione (TPD), thieno[3,4-b]thiophene (TT), or pyrrolo[3,4-c]pyrrole-1,4-dione (DPP) unit on the polymer backbone was demonstrated. All three new random copolymers, RP1, RP2 and RP3, displayed broad absorption bands and lower optical band gaps compared to those of their parent alternating polymer, PBDTT-DPPD. The estimated band gaps of RP1, RP2 and RP3 decreased gradually from 2.04 eV for PBDTT-DPPD to 1.87 eV, 1.60 eV and 1.45 eV, respectively. The decrease in the band gaps of RP1, RP2 and RP3 was associated mainly with the alteration of their conduction bands. Interestingly, RP1 and RP2 showed slightly improved hole mobility and RP3 exhibited one order lower hole mobility than that of PBDTT-DPPD. The estimated mobilities of RP1, RP2 and RP3 were 1.4 x 10^{-3} $cm^2V^{-1}s^{-1}$, 3.7 x 10^{-3} $cm^2V^{-1}s^{-1}$ and 4.9 x 10^{-4} $cm^2V^{-1}s^{-1}$, respectively. The polymer solar cells (PSCs) prepared from RP1, RP2 or RP3 as an donor and $PC_{70}BM$ as an acceptor using a simple device configuration of ITO/PEDOT:PSS/polymer:$PC_{70}BM$+DIO/Al exhibited a maximum power conversion efficiency (*PCE*) of 5.35%, 5.05% and 2.41%, respectively.

1. Introduction

Polymer solar cells (PSCs) are one of the most promising clean and renewable energy production technologies because of their high solar to electrical energy conversion efficiency, light weight, flexibility, and easy device fabrication via solution processability to large areas.[1,2] In PSCs, a photoactive layer used for light harvesting and charge separation is crucial for the solar to electrical energy conversion efficiency, and the blends of π–conjugated polymer and fullerene derivative are used widely for its preparation.[1,2] The power conversion efficiency (*PCE*) of traditional single layer PSCs is improved to more than 10%[3,4] by changing the opto-electrical and charge transport properties of the photoactive layer via the utilization of different structured π–conjugated polymers[5-8] and fullerene derivatives,[9-11] as well as by controlling the morphology of the photoactive layer using different processive additive materials.[12,13] Tandem or multilayer PSCs were also reported to improve the *PCE*.[14-19] In the latter case, the use of two or more π–conjugated polymers and fullerene derivatives in the preparation of the photoactive layers increased the light harvesting ability and maximized the voltage. Consequently, multilayer PSCs showed improved photovoltaic performance compared to single layer PSCs.[14-19] However, the maximum *PCE* (~11.5%) of multilayer PSCs[14] was not improved greatly compared to that of single layer PSCs (*PCE* ~10.6%).[3,4,20-22] Note that multilayer PSCs device fabrication is much more difficult than that of single layer PSCs. Recently, ternary blend PSCs were reported to overcome the device fabrication difficulties.[23,24] In ternary blend PSCs, two or more polymers displaying their absorption bands at different intervals of solar spectra were used on the photoactive layer. However, the overall *PCE* is lower than that of single or multilayer PSCs and the reported maximum *PCE* of ternary blend PSCs was 8.6%.[23,24] Those results showed that the device architecture of single layer PSCs is better than that of multilayer or ternary blend PSCs because of its easy device fabrication and high *PCE*. To increase the *PCE* of single layer PSCs further, chemists have made efforts to prepare broad absorbing and low band gap electron donating π-conjugated polymers or efficient electron accepting fullerene derivatives. This study examined the preparation of those π-conjugated polymers for PSCs.

The convenient way of preparing those polymers is to make donor-acceptor (D-A) alternating polymers or ternary (or

---

[a] *Department of Chemistry, Chemistry Institute for Functional Materials, Pusan National University, Busan 690-735, Repub-lic of Korea. Fax: 82-51-516-7421; Tel: 82-51-510-2245; E-mail: mhhyun@pusan.ac.kr*

[b] *Department of Physics, Pukyong National University, Busan 608-737, Republic of KoreaAddress, Address, Town, Country. Fax: 82-51-629-5549; Tel: 82-51-629-5774; E-mail: spark@pknu.ac.kr*

[c] *Department of Physics and EHSRC, University of Ulsan, Ulsan 680-749, Republic of Korea*

[d] *Department of Industrial Chemistry, Pukyong National University, Busan 608-739, Republic of Korea.*

random) copolymers via the random copolymerization of three different units. According to the literatures, D-A polymers containing electron deficient 2,1,3-bezothiadiazole (BT) units displayed broad absorption bands from 300 nm to 800 nm.[25-27] On the other hand, the D-A polymers containing electron deficient units, such as thieno[3,4-c]pyrrole-4,6-dione (TPD),[28,29] thieno[3,4-b]thiophene (TT)[20-22] and pyrrolo[3,4-c]pyrrole-1,4-dione (DPP),[19,30,31] exhibit impressive photovoltaic performances compared to BT based polymers, even though those polymers display an intense absorption band only at the low energy part of the solar spectrum (500-800 or 900 nm). The insertion of a weak electron accepting unit, which was shown to afford highly efficient large band gap polymers when polymerized with electron rich units, in the backbone of TPD or TT or DPP-based polymers might give broad absorbing low band gap polymers. Recently, one of the alternating polymers (PBDTT-DPPD, shown in Fig. 1) containing electron rich 2D-conjugated benzodithiophene (BDTT) and novel electron deficient pyrrolo[3,4-c]pyrrole-1,3-dione (DPPD) derivatives was found to show excellent photovoltaic parameters such as a maximum *PCE* of 6.57% with an open-circuit voltage (V_{oc}) of 0.90 V, a short-circuit current (J_{sc}) of 10.12 mA/cm^2, a fill factor (*FF*) of 72%, and an incident photon to current efficiency (*IPCE*) of 73% (>70% *IPCE* response from 360 nm to 500 nm) for simple structured PSCs.[32] The BDTT-based D-A alternating polymer containing the DPPD unit displayed a large band gap (~2.04 eV),[32] while those incorporating each of TPD, TT and DPP units showed lower band gaps (~1.88 eV, 1.59 eV and 1.44 eV, respectively.).[20-22,28-31] On the other hand, all four alternating polymers, such as PBDTT-DPPD, PBDTT-TPD, PBDTT-TT, and PBDTT-DPP gave high *PCE* when they were used as an electron donor material in PSCs.[20-22,28-31] The chemical structures and band gaps of PBDTT-DPPD, PBDTT-TPD, PBDTT-TT, and PBDTT-DPP are presented in Fig. 1. As stated earlier, the incorporation of TPD, TT and DPP units in the PBDTT-DPPD backbone is expected to reduce its band gap gradually and is expected to give a high J_{sc} and *PCE*.

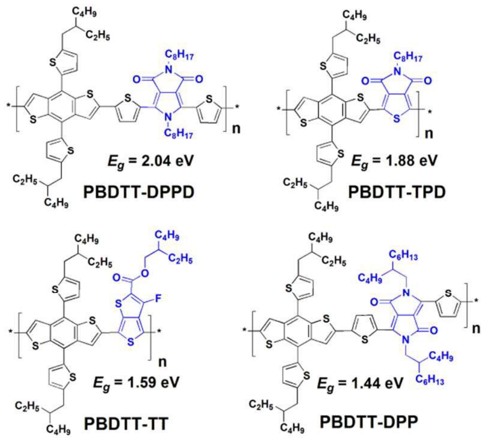

Fig. 1. Chemical structures of highly efficient large ban gap polymer PBDTT-DPPD and low band gap polymers PBDTT-TPD, PBDTT-TT and PBDTT-DPP.

In this instance, we prepared three new random copolymers, such as RP1, RP2 and RP3 containing BDTT, DPPD and one of the TPD, DPP and TT units, respectively. This paper briefly discusses the opto-electrical, charge transport and photovoltaic properties modulation of PBDTT-DPPD via the incorporation of relatively strong electron accepting units such as TPD, TT and DPP on its backbone.

2. Experimental section

2.1 Materials and Instruments

The reagents and solvents were purchased from Sigma-Aldrich. The nuclear magnetic resonance (NMR) spectra of the polymers were recorded on a Varian Mercury Plus spectrometer (300 MHz). The molecular weights of the polymers were determined by permeation chromatography (GPC) on an Agilent 1200 Infinity Series separation module gel with chloroform as an eluent at ambient temperature. The GPC instrument was calibrated with a polystyrene standard prior to analysis. Thermogravimetric analysis (TGA) of the polymers was performed on a TA instrument Q600-0825 at a heating and cooling rate of 10 °C/min under nitrogen. The UV-visible near infrared (NIR) absorption spectra of the polymers in the solution and film state were recorded on a JASCO V-570 spectrophotometer. Cyclic voltammetry (CV) of the polymers was conducted on a CH Instruments Electrochemical Analyzer. Three electrode (polymer cast platinum as a working electrode, Ag/AgCl as a reference electrode and platinum wire as a counter electrode in an acetonitrile solution containing 0.1 M tetrabutylammonium tetrafluoroborate (Bu_4NBF_4) as the supporting electrolyte) electrochemical systems were used for CV analysis and the CV instrument was calibrated to the ferrocene/ferrocenium ion (Fc/Fc$^+$) standard. Atomic force microscopy (AFM) was performed using Seiko instruments (SPI 3800N-SPA 400).

2.2 Fabrication and characterization of OFETs

The organic field effect transistors (OFETs) were fabricated on highly n-type-doped silicon (Si) substrates with a 200 nm layer of thermally grown silicon oxide (SiO_2). The Si substrates were subjected to an UV-Ozone treatment for 30 min and then treated with an octadecyltrichlorosilane (OTS) self-assembled monolayer. The n-type doped Si substrate functions as a gate electrode and the SiO_2 layer acts as a gate dielectric. The chlorobenzene (CB) solution of the polymer (10 mg/ml) was spin-cast on top of the Si substrate (2000 rpm) and then dried at room temperature (RT) for 30 min. The source and drain electrodes (Au, 70 nm) were deposited on top of the polymer layer by thermal evaporation in a vacuum of approximately 2 x 10^{-6} Torr. The channel length (L) and channel width (W) of the device was 50 μm and 3.0 mm, respectively. The output and transfer characteristics of the OFETs were measured by using a Keithley semiconductor parametric analyzer (Keithley 4200). All preparation processes and characterization of the OFETs were performed inside a N_2-atmosphere glove box.

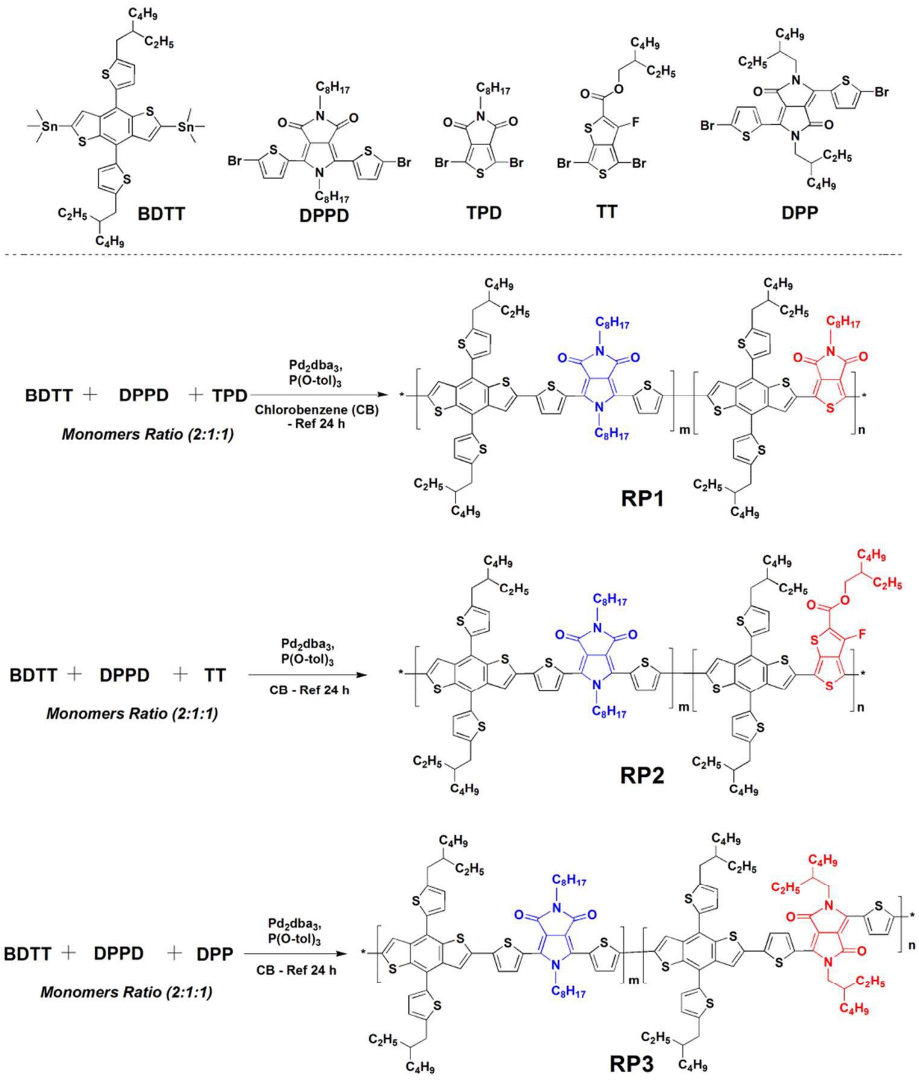

Scheme 1 Synthetic route to polymers RP1, RP2 and RP3.

The mobility (μ) was determined using the following equation in the saturation regime:

$$I_{DS,sat} = (\mu W C_i/2L)\,(V_{GS}-V_T)^2$$

where C_i is the capacitance per unit area of the SiO_2 dielectric (C_i = 15 nF cm^{-2}) and V_T is the threshold voltage.

2.3 Fabrication and characterization of PSCs

The PSCs were fabricated with the simple device structure of ITO-coated glass substrate/PEDOT:PSS/polymer:$PC_{70}BM$/Al. A pre-cleaned ITO-coated glass substrate was dried overnight in an oven. Subsequently, a 40 nm thick layer of PEDOT:PSS (Baytron PH) was spin-cast from an aqueous solution on an ITO-coated glass substrate. The substrate was dried for 10 min at 140 °C in air and then transferred to a glove box to spin-cast the photoactive layer. A solution containing a mixture of polymer:$PC_{70}BM$ (1.0:1.0, 1.0:1.5, 1.0:2.0, 1.0:2.5 and 1.0:3.0 wt%) in CB:1,8-diiodoctane (DIO) (97:3 vol%) with a total concentration of 20 mg/ml was then spin-cast on top of the PEDOT/PSS layer. The film was dried for 30 min at RT in a glove box. An aluminium (Al, 100 nm) electrode was then deposited by thermal evaporation in a vacuum of approximately 3 x 10^{-6} Torr. The current density-voltage (*J*–*V*) characteristics of the PSC devices were measured using a Keithley 2400 Source Measure Unit. The solar cell performance utilized an Air Mass 1.5 Global (AM 1.5 G) solar simulator with an irradiation intensity of 1000 Wm^{-2}. The spectral mismatch factor was calculated by a comparison of the solar simulator spectrum with the AM 1.5 spectrum at RT.

2.4 Synthesis of polymers

Monomers BDTT,[32] DPPD,[32,33] TPD,[29] TT[21] and DPP[30] were prepared using similar procedures to those reported elsewhere, and random copolymers namely RP1, RP2 and RP3 were synthesized via the Stille polycondensation reaction, as described below.

2.4.1. Synthesis of RP1

BDTT (0.27 g, 0.30 mmol), DPPD (0.10 g, 0.15 mmol) and TPD (0.06 g, 0.15 mmol) were added to a flame dried three-neck round bottom flask equipped with a magnetic bar, a condenser rubber septum, and stopper. CB (20 mL) was then added using a syringe through the rubber septum and the solid materials were dissolved completely. The solution was purged with argon for 30 min and $Pd_2(dba)_3$ (14 mg) and $P(o\text{-}tol)_3$ (30 mg) were added in one portion to the degassed solution. The mixture was stirred and heated to reflux under an argon atmosphere for 24 h. The solution was cooled to RT and then added drop-wise to a vigorously stirred methanol (200 mL). The precipitates were recovered by filtration, and the crude polymer was extracted with methanol and acetone for 24 h in a Soxhlet apparatus to afford pure polymer RP1: Dark brown solid. Yield (0.27 g, 94%). ^1H NMR (300 MHz, $CDCl_3$): δ 7.74 (s, 4H), 7.30-7.60 (m, 6H), 6.97 (s, 6H), 4.40 (s, 2H), 3.60 (s, 4H), 2.80-3.20 (m, 8H), 0.60-2.00 (m, 105H). Anal. Calcd for $C_{112}H_{137}N_3O_4S_{11}$: C, 69.27; H, 7.11; N, 2.16; S, 18.16. Found: C, 68.02; H, 6.64; N, 1.59; S, 16.68.

2.4.2. Synthesis of RP2

RP2 was prepared using a similar synthetic procedure to that used for the synthesis of RP1. In this reaction, monomers BDTT (0.27 g, 0.3 mmol), DPPD (0.10 g, 0.15 mmol) and TT (0.07 g, 0.15 mmol) were taken for polymerization. RP2: Black color. Yield (0.29 g, 97%). ^1H NMR (300 MHz, $CDCl_3$): δ 7.60-8.20 (m, 4H), 7.30-7.60 (m, 6H), 6.97 (s, 6H), 4.32 (s, 4H), 3.60 (s, 2H), 2.80-3.20 (m, 8H), 0.60-2.00 (m, 105H). Anal. Calcd for $C_{113}H_{137}FN_2O_4S_{12}$: C, 68.16; H, 6.94; N, 1.41; S, 19.33. Found: C, 66.97; H, 6.70; N, 1.06; S, 18.89.

2.4.3. Synthesis of RP3

RP3 was prepared using a similar synthetic procedure used for the synthesis of RP1. In this reaction, monomers BDTT (0.27 g, 0.3 mmol), DPPD (0.10 g, 0.15 mmol) and DPP (0.10 g, 0.15 mmol) were taken for polymerization. RP3: Black color. Yield (0.31 g, 94%). ^1H NMR (300 MHz, $CDCl_3$): δ 8.80-9.40 (m, 2H), 7.74 (s, 4H), 7.36 (s, 8H), 6.97 (s, 6H), 4.42 (s, 2H), 4.04 (s, 4H), 3.60 (s, 2H), 2.80-3.20 (m, 8H), 0.60-2.00 (m, 120H). $C_{128}H_{158}N_4O_4S_{12}$: C, 69.84; H, 7.23; N, 2.55; S, 17.48. Found: C, 68.87; H, 6.78; N, 2.08; S, 16.91.

3. Results and discussions

3.1 Synthesis and characterization of polymers

The synthetic route for the preparation of random copolymers RP1, RP2 and RP3 are outlined in Scheme 1. All three polymers were prepared using Stille polymerization between the respective monomers shown in Scheme 1. The weight average (M_w)/number average (M_n) molecular weights of RP1, RP2 and RP3 determined by GPC analysis were 2.16 × 10^4 $gmol^{-1}$/0.94 × 10^4 $gmol^{-1}$, 1.99 × 10^4 $gmol^{-1}$/1.12 × 10^4 $gmol^{-1}$ and 6.97 × 10^4 $gmol^{-1}$/1.82 × 10^4 $gmol^{-1}$, respectively. The calculated polydispersities (PDI, M_w/M_n) were 2.29, 1.78 and 3.82, respectively. All three copolymers, RP1, RP2 and RP3, showed moderate solubility in chloroform and very good solubility in CB and dichlorobenzene (DCB). The m:n ratio of each copolymer determined from its NMR spectra was ~1:1. The 5% weight loss temperatures determined from TGA were above 400 °C. The thermal stability of the polymers, RP1, RP2 and RP3, was similar to that of their parent alternating polymers, such as PBDTT-DPPD[32] and PBDTT-TPD[28,29] or PBDTT-TT[20-22] or PBDTT-DPP,[30,31] respectively. The latter results suggest that the incorporation of TPD, TT and DPP units in the main chain of PBDTT-DPPD does not make any significant change to its thermal stability. The molecular weights of PBDTT-DPPD, RP1, RP2 and RP3 are presented in Table 1.

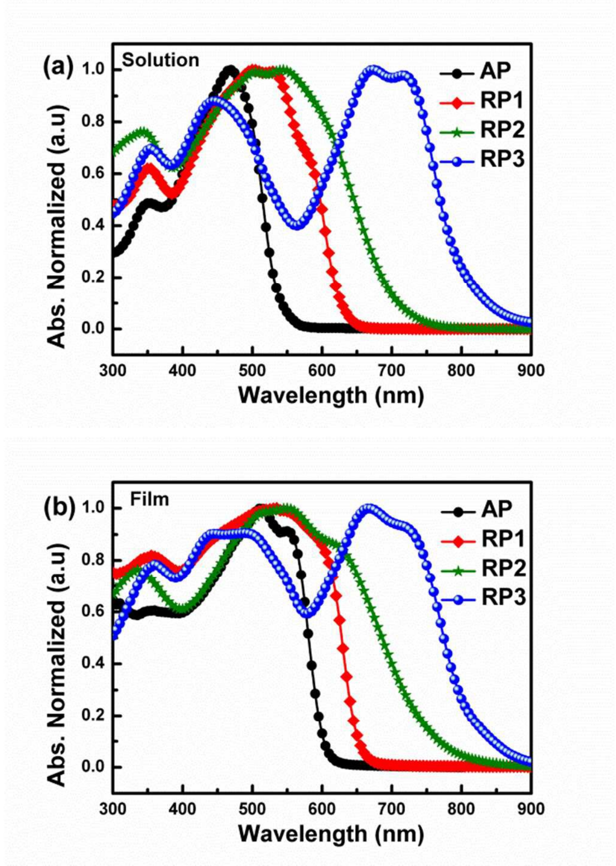

Fig. 2 Absorption spectra of polymers PBDTT-DPPD = AP, RP1, RP2 and RP3.

3.2 Optical properties

The UV-Vis NIR absorption spectra of alternating polymer, PBDTT-DPPD, and new random copolymers, RP1, RP2 and RP3, are shown in Fig. 2a (in chloroform) and Fig. 2b (as thin film on glass). All three copolymers, RP1, RP2 and RP3, displayed red shifted absorption bands compared to that of PBDTT-DPPD in both the solution and film state. The absorption maxima of copolymers, RP1, RP2 and RP3, are presented in Table 1 and those were found to be red shifted by 21 nm, 38 nm and 153 nm, respectively, for RP1, RP2 and RP3 compared to that of PBDTT-DPPD. The estimated optical band gaps (E_g) of RP1, RP2 and RP3 were 1.87 eV, 1.60 eV and 1.45 eV, respectively, using the onset absorption wavelength in the film. Each of the copolymers, RP1, RP2 and RP3, showed a distinct absorption band and E_g due to the different electron accepting ability of the TPD, TT and DPP units. The electron accepting ability of the electron deficient units used in this study was expected to be in the order of DPPD<TPD<TT<DPP, and consequently, polymers exhibited a band gap in the order of PBDTT-DPPD >RP1>RP2>RP3. A comparison of the absorption bands of copolymers, RP1, RP2 and RP3, with their corresponding parent alternating polymers, such as PBDTT-DPPD,[32] PBDTT-TPD,[28,29] PBDTT-TT,[20-22] and PBDTT-DPP[30,31] showed that the absorption bands can be attributed to a combination of the absorption spectra of PBDTT-DPPD and PBDTT-TPD or PBDTT-TT or PBDTT-DPP, respectively. The band gaps of the copolymers, RP1, RP2 and RP3, are consistent with those of the alternating polymers (repeating unit "n") PBDTT-TPD ($E_g \sim$ 1.88 eV), PBDTT-TT ($E_g \sim$ 1.59 eV) and PBDTT-DPP ($E_g \sim$ 1.44 eV), respectively, and also displayed strong absorption at the high energy part of the solar spectrum (300-600 nm) due to the presence of a weak electron accepting DPPD unit on its backbone. The optical properties of PBDTT-DPPD, RP1, RP2 and RP3 are summarized in Table 1.

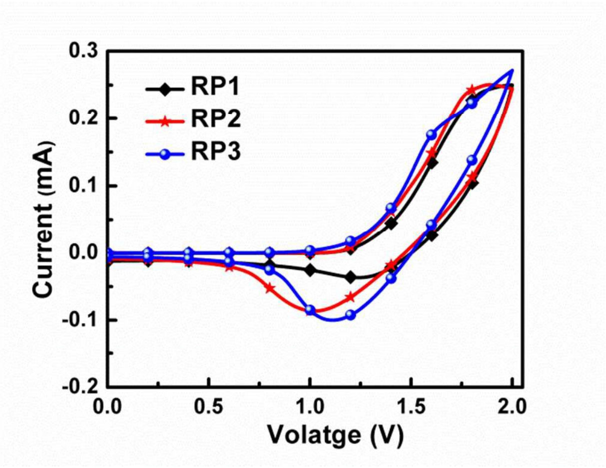

Fig. 3 Cyclic voltammograms of polymers RP1, RP2 and RP3.

3.3 Electrochemical properties

The highest occupied/lowest unoccupied molecular orbital (HOMO/LUMO) energy levels of the copolymers, RP1, RP2 and RP3, were determined by CV analysis. CV spectra of the copolymers, RP1, RP2 and RP3, are presented in Fig. 3. The HOMO/LUMO levels of the copolymers, RP1, RP2 and RP3, were estimated to be –5.38 eV/–3.51 eV, –5.36 eV/–3.76 eV and –5.31 eV/–3.86 eV, respectively, using the standard equations shown below $E_{\mathrm{HOMO}} = [-(E_{\mathrm{ox,onset\ vs.\ Ag/AgCl}} - E_{\mathrm{ferrocene\ vs.\ Ag/AgCl}}) - 4.8]$ eV and LUMO = HOMO+E_g.[33-35] The $E_{\mathrm{ox,onset\ vs.\ Ag/AgCl}}$ values of the copolymers, RP1, RP2 and RP3, calculated from Fig. 3 were 1.18 V, 1.16 V and 1.11 V, respectively, and the $E_{\mathrm{ferrocene\ vs.\ Ag/AgCl}}$ was 0.60 V. Comparisons of the HOMO/LUMO energy levels of the copolymers, RP1, RP2 and RP3, with their corresponding parent alternating polymers, such as PBDTT-DPPD (–5.44 eV/–3.40 eV)[32] and PBDTT-TPD (–5.34 eV/–3.46 eV)[28,29] or PBDTT-TT (–5.19 eV/–3.25 eV)[20-22] or PBDTT-DPP (–5.30 eV/–3.63 eV),[30,31] respectively, suggest that the insertion of electron accepting units, such as TPD, TT and DPP, on the PBDTT-DPPD backbone mainly reduces its conduction band. However, all three copolymers, RP1, RP2 and RP3, showed sufficient energy differences (>0.44 eV) between the LUMO levels of the polymer and $PC_{70}BM$ for efficient electron transfer from the polymer to $PC_{70}BM$. In addition, the HOMO energy levels of all three copolymers, RP1, RP2 and RP3, were found to be deep enough to obtain a high V_{oc} when used in PSCs. The HOMO and LUMO energy levels of PBDTT-DPPD, RP1, RP2 and RP3 are summarized in Table 1.

3.4 OFETs characteristics

The hole mobilities of the random copolymers, RP1, RP2 and RP3, were estimated by making OFETs with each copolymer to understand the charge transport modulation of PBDTT-DPPD by the insertion of TPD, TT and DPP units. All three copolymers, RP1, RP2 and RP3, were found to be p-type semiconducting polymers from the respective OFET characteristics shown in Fig. 4 (a, c, e), and the estimated hole mobilities (μ) of RP1, RP2 and RP3 were 1.4 x 10^{-3} $cm^2V^{-1}s^{-1}$, 3.7 x 10^{-3} $cm^2V^{-1}s^{-1}$ and 4.9 x 10^{-4} $cm^2V^{-1}s^{-1}$, respectively, from the OFET curves shown in Fig. 4 (b, d, f). Note that the reported hole mobilities of the parent alternating polymers, PBDTT-DPPD,[32] PBDTT-TPD,[28,29] PBDTT-TT,[20-22] and PBDTT-DPP,[30,31] were 1.0 x 10^{-3} $cm^2V^{-1}s^{-1}$, 4.7 x 10^{-4} $cm^2V^{-1}s^{-1}$, 1.7 x 10^{-4} $cm^2V^{-1}s^{-1}$, and 3.1 x 10^{-4} $cm^2V^{-1}s^{-1}$ respectively. A comparison of the hole mobilities of the copolymers, RP1, RP2 and RP3, with that of PBDTT-DPPD showed that the incorporation of TPD or TT units does not make any significant changes to its charge transport behaviours, but at the same time, the incorporation of DPP unit reduces its hole mobility by one order of magnitude. These results suggest that the structural disorder originated from the insertion of second electron acceptor unit on the PBDTT-DPPD backbone is pronounced in RP3 while almost zero in RP1 and RP2. The electron accepting imide or thienyl group was attached as the side chain on the backbone of the electron rich thiophene of TPD and TT units and, consequently, the incorporation of electron deficient TPD or TT unit on the PBDTT-DPPD backbone was expected to maintain or improve its planarity and molecular packing slightly, which leads the higher hole mobility. In contrast, the presence of electron accepting groups on the backbone of the DPP unit and the large structural difference between the DPP and DPPD units allow the considerable structural disorder of the copolymer, which notably lowers the hole mobility. On the other hand, the hole mobilities of RP1 and RP2 were one order higher than that of the alternating polymers, PBDTT-TPD and PBDTT-TT, respectively, and RP3 showed similar hole mobility to that of PBDTT-DPP. DPPD-based polymers were proved to exhibit higher hole mobilities than TPD, TT and DPP-based polymers and, consequently, random copolymers showed higher hole mobility than PBDTT-TPD, PBDTT-TT and PBDTT-DPP.[36] The hole mobilities of PBDTT-DPPD, RP1, RP2 and RP3 are included in Table 1.

Table 1 Polymerization Results, Thermal, Optical and Electrochemical properties of polymers PBDTT-DPPD, RP1, RP2 and RP3.

Polymer[a]	M_w[b] (x10^4 g/mol)	PDI[b]	λ_{max} as sol (nm)[c]	λ_{max} as film (nm)[d]	E_g (eV)[e]	HOMO (eV)[f]	LUMO (eV)[g]	μ ($cm^2V^{-1}s^{-1}$)[h]
PBDTT-DPPD	3.72	2.01	467	514	2.04	−5.44	−3.40	1.0 x 10^{-3}
RP1	2.16	2.29	503	535	1.87	−5.38	−3.51	1.4 x 10^{-3}
RP2	1.99	1.78	546	552	1.60	−5.36	−3.76	3.7 x 10^{-3}
RP3	6.97	3.82	443, 674	494, 667	1.45	−5.31	−3.86	4.9 x 10^{-4}

[a] Data for PBDTT-DPPD are quoted from reference 32. [b] Weight average molecular weight (M_w) and polydispersity (PDI) of the polymers were determined by GPC using polystyrene standards. [c] Measurements were performed in chloroform. [d] Measurements in thin film were performed on the glass substrate. [e] Band gap estimated from the onset wavelength of the optical absorption in thin film. [f] The HOMO level was estimated from cyclic voltammetry analysis. [g] The LUMO level was estimated by using the following equation: LUMO = HOMO + E_g. [h] The hole mobility of polymers were estimated from organic field effect transistors.

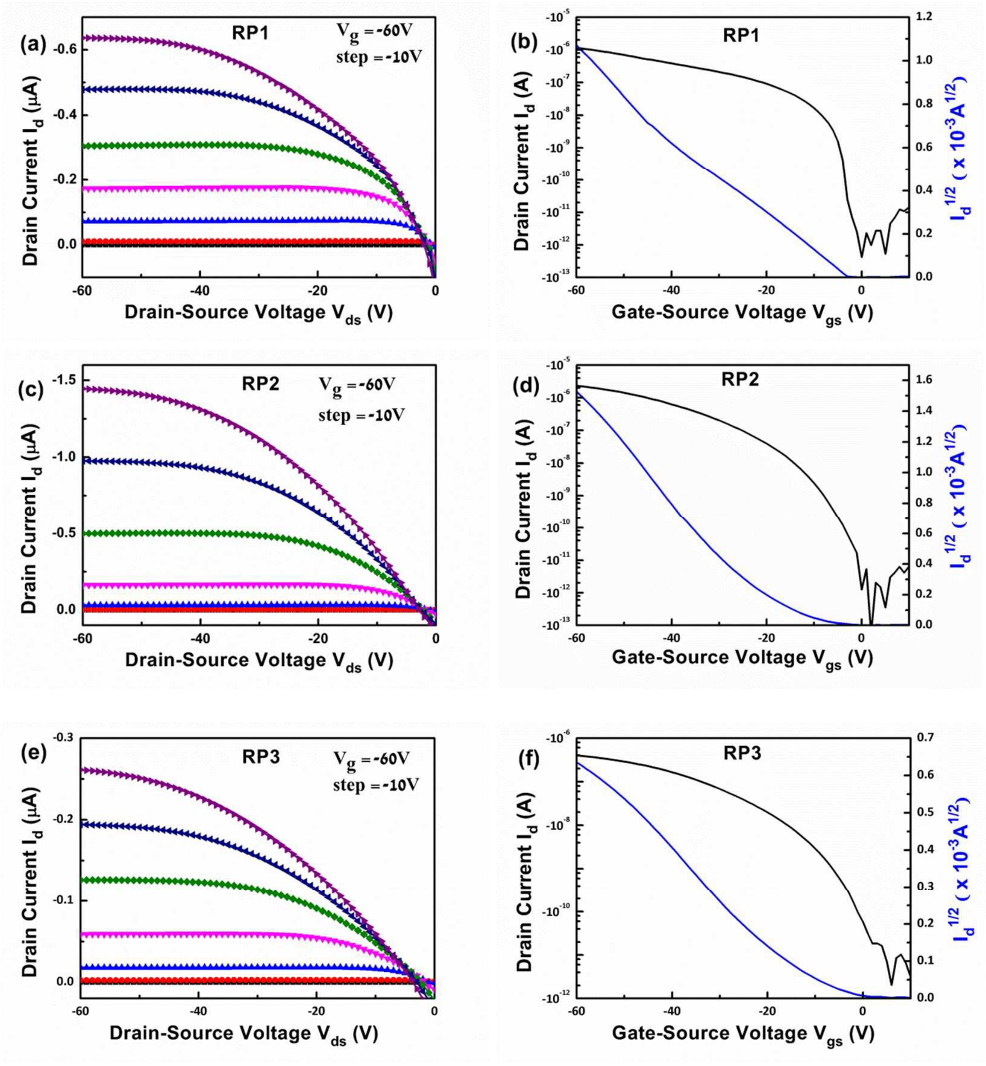

Fig. 4 Typical current-voltage characteristic (drain-source current, I_{DS}, Vs drain-source voltage, V_{DS}) at different voltage (a, c and e, respectively.) and I_{DS} and $I_{DS}^{1/2}$ Vs V_{GS} plots at V_{DS} of −60 V (b, d and f, respectively.) for RP1-, RP2- and RP3-based OFET devices.

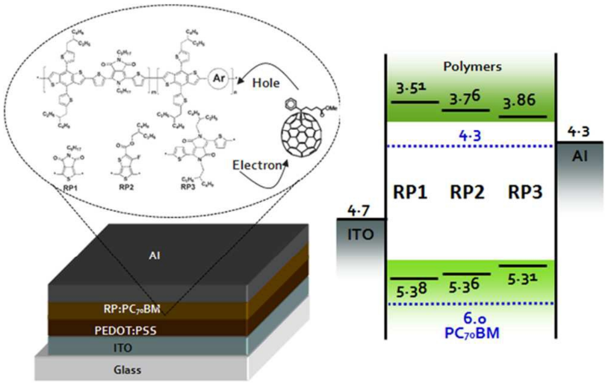

Fig. 5 Device structure and energy levels diagram of PSCs.

3.5 Photovoltaic Properties

To compare the photovoltaic performances of RP1, RP2 and RP3 with the parent alternating polymer, PBDTT-DPPD, PSCs were fabricated with a configuration of (ITO/PEDOT:PSS/polymer:$PC_{70}BM$/Al), which was used in our previous study.[32] The device structure of the PSCs used in this study is illustrated in Fig. 5 along with the energy levels. The current-voltage (*J–V)* characteristics of the PSCs prepared using each random copolymer, RP1, RP2 and RP3, as an electron donor and $PC_{70}BM$ as an electron acceptor with 3 vol% 1,8-diiodoocatne (DIO) are presented in Fig. 6. The *J–V* curves were measured under an illumination of an AM 1.5 G (100 $mWcm^{-2}$) solar simulator and their corresponding photovoltaic parameters are summarized in Table 2. The PSCs made from RP1:$PC_{70}BM$ (1.0:1.5 wt%)+3 vol% DIO, RP2:$PC_{70}BM$ (1.0:1.0 wt%)+3 vol% DIO and RP3:$PC_{70}BM$ (1.0:2.0 wt%)+3 vol% DIO blends exhibited a maximum *PCE* of 4.50% (V_{oc} ~ 0.90 V, J_{sc} ~ 8.11 mA/cm^2, and *FF* ~ 61%), 5.05% (V_{oc} ~ 0.80 V, J_{sc} ~ 10.90 mA/cm^2, and *FF* ~ 58%) and 2.41% (V_{oc} ~ 0.66 V, J_{sc} ~ 7.71 mA/cm^2, and *FF* ~ 47%), respectively. Copolymers RP1 and RP3 displayed a much lower photocurrent than that of the parent alternating polymer, PBDTT-DPPD (J_{sc} = 10.12 mA/cm^2), although the former copolymers showed broader absorption bands and lower band gaps than PBDTT-DPPD.

PSCs with a higher total concentration (25 mg/mL) of copolymer:$PC_{70}BM$ (1:1.5 wt%)+3 vol% DIO blend solution were also fabricated to improve the photocurrent. The respective *J–V* curves are shown in Fig. 7a and their corresponding photovoltaic parameters are summarized in Table 3. As expected, the photo-current and fill factor of the PSCs made from RP1 were improved significantly when the photoactive layer thickness was increased. However, the notably lowered V_{oc} (0.14 V) limits its *PCE* to 5.35% (V_{oc} = 0.76 V, J_{sc} = 10.60 mA/cm^2, and *FF* = 67%). On the other hand, the photovoltaic parameters of the PSC made from RP2 were not significantly changed when the photoactive layer thickness was increased. RP2-based PSC offered a *PCE* = 4.73% (V_{oc} = 0.75 V, J_{sc} = 10.90 mA/cm^2, and *FF* = 58%). The PSC prepared from RP3 showed a higher current, lower V_{oc} and *FF*, which leads to a lower *PCE* of 2.21% (V_{oc} = 0.63 V, J_{sc} = 10.30 mA/cm^2, and *FF* = 34%). In general, when the photoactive layer thickness of PSCs was increased, the photo-current was enhanced considerably, but the photo-voltage was reduced notably for all the copolymers. Consequently, a large difference was not seen in their overall photovoltaic performances.

To understand the additive influences on the performances of PSCs, PSCs were also prepared using copolymer:$PC_{70}BM$ (1:1.5 wt%) blend solution with 3 vol% diphenyl ether (DPE) as an additive. The respective *J–V* curves are shown in Fig. 7b and their results are presented in Table 3. The devices made with DPE showed similar performances to those of the devices made with DIO. All three copolymers, RP1, RP2 and RP3, exhibited a similar photo-current although each copolymer showed a quite different absorption band. In addition, copolymers RP1, RP2 and RP3 offered only a slightly higher photo-current although their absorption bands were much broader than that of PBDTT-DPPD. To understand why, the incident photon to collected electron (*IPCE*) spectra of the PSCs made from copolymer:$PC_{70}BM$ (25 mg/ml, 1:1.5 wt%)+3 vol% DIO blends were measured. The *IPCE* spectra of the PSCs are displayed in Fig. 8. The *IPCE* spectra of the PSCs extended from 300 nm to 700 nm or 750 nm or 800 nm, respectively, for the RP1-, RP2- and RP3-based PSCs, which is similar to that of the absorption bands of the copolymers.

Table 2 Photovoltaic Properties of the Polymer Solar Cells Prepared by Using the Configuration of ITO/PEDOT:PSS/polymer:$PC_{70}BM$(20 mg/mL)+ 3 vol% DIO/Al.

Polymer:$PC_{70}BM$ ratio	J_{sc} (mA/cm^2)^a	V_{oc} (V)^b	FF (%)^c	PCE (%)^d
RP1:$PC_{70}BM$ (1.0:1.0 wt%)	7.38	0.89	55	3.58
RP1:$PC_{70}BM$ (1.0:1.5 wt%)	8.11	0.90	61	4.50
RP1:$PC_{70}BM$ (1.0:2.0 wt%)	6.61	0.91	61	3.68
RP1:$PC_{70}BM$ (1.0:2.5 wt%)	3.43	0.90	67	2.07
RP2:$PC_{70}BM$ (1.0:1.0 wt%)	10.90	0.80	58	5.05
RP2:$PC_{70}BM$ (1.0:1.5 wt%)	10.67	0.81	58	4.99
RP2:$PC_{70}BM$ (1.0:2.0 wt%)	10.11	0.81	61	5.01
RP2:$PC_{70}BM$ (1.0:2.5 wt%)	7.48	0.82	62	3.77
RP3:$PC_{70}BM$ (1.0:1.0 wt%)	3.92	0.71	47	1.31
RP3:$PC_{70}BM$ (1.0:2.0 wt%)	7.71	0.66	47	2.41
RP3:$PC_{70}BM$ (1.0:3.0 wt%)	7.26	0.70	41	2.06

[a] Short-circuit current density. [b] Open-circuit voltage. [c] Fill factor. [d] Power conversion efficiency.

Table 3 Photovoltaic Properties of the Polymer Solar Cells Prepared by Using the Configuration of ITO/PEDOT:PSS/polymer:$PC_{70}BM$(25 mg/Ml, 1:1.5 wt%)+ 3 vol% DIO or DPE/Al.

Polymer	Additive	J_{sc} (mA/cm^2)^a	V_{oc} (V)^b	FF (%)^c	PCE (%)^d
RP1	DIO	10.60	0.76	67	5.35
RP2	DIO	10.90	0.75	58	4.73
RP3	DIO	10.30	0.63	34	2.21
RP1	DPE	10.70	0.75	65	5.21
RP2	DPE	10.90	0.75	60	4.90
RP3	DPE	9.67	0.66	33	2.14

[a] Short-circuit current density. [b] Open-circuit voltage. [c] Fill factor. [d] Power conversion efficiency.

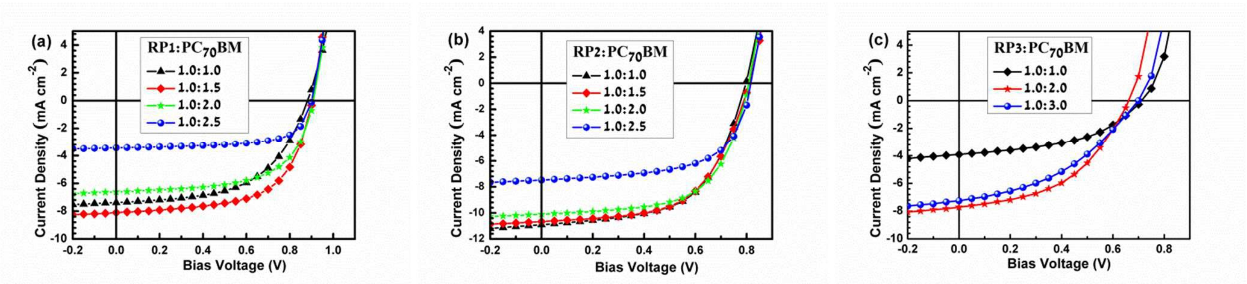

Fig. 6 *J–V* characteristics of the PSCs made from RP1 (a), RP2 (b) and RP3 (c), respectively, using the device structure of ITO/PEDOT:PSS/Polymer:$PC_{70}BM$(20 mg/mL)+3 vol% DIO/Al.

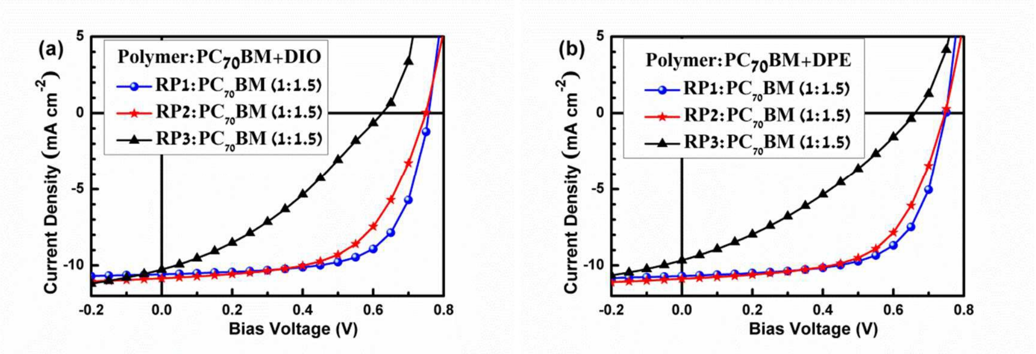

Fig. 7 *J–V* characteristics of the PSCs made from RP1, RP2 and RP3 with a device structure of ITO/PEDOT:PSS/Polymer:$PC_{70}BM$(25 mg/mL)+3 vol% DIO/Al (a) and ITO/PEDOT:PSS/Polymer:$PC_{70}BM$(25 mg/mL)+3 vol% DPE/Al (b).

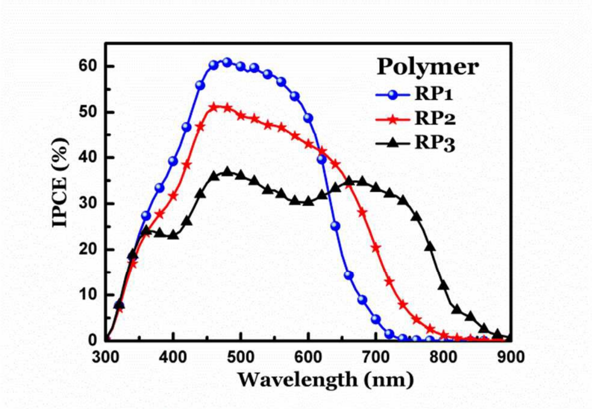

Fig. 8 IPCE spectra of the PSCs made from RP1, RP2 and RP3, respectively, using the device structure of ITO/PEDOT:PSS/Polymer:$PC_{70}BM$(25 mg/mL)+3 vol% DIO/Al.

As expected, the new copolymer-based PSCs displayed a broader *IPCE* response than the PBDTT-DPPD-based PSC, but at the same time, the *IPCE* maxima of the new copolymer-based PSCs were notably lower than that of the PBDTT-DPPD-based PSC. Consequently, the new copolymer-based PSCs offered only a slightly improved photocurrent compared to that of the PBDTT-DPPD-based PSC.

The surface morphology of the photoactive layer is the crucial determining factor for PSC device performance. Therefore, the morphologies of the films made from copolymer:$PC_{70}BM$ (25 mg/ml, 1:1.5 wt%) blends without and with 3 vol% DIO were examined by AFM. The respective tapping (a and c) and phase (b and d) mode AFM images are shown in Fig. 9. Note that images a and b were obtained for the films prepared without DIO and images c and d were obtained for the film prepared with 3 vol% DIO. The films made without DIO exhibited poor morphologies for all three copolymers. On the other hand, the films made with 3 vol% DIO exhibited improved blending between the copolymer and $PC_{70}BM$ and the roughness was much lower as well. The morphologies of the films prepared from all three copolymers, RP1, RP2 and RP3, were ideal for efficient electron transport from the polymer to $PC_{70}BM$. However, RP3 displayed a very different morphology compared to that of RP1 and RP2. The latter phenomenon and lower hole mobility of RP3 could explain its poor photovoltaic performance compared to that of RP1 and RP2.

A comparison of the photovoltaic parameters obtained in this study for copolymers RP1 (*PCE* = 5.35%, J_{sc} = 10.60 mA/cm^2, V_{oc} = 0.76 V, and *FF* = 67%), RP2 (*PCE* = 5.05%, J_{sc} = 10.90 mA/cm^2, V_{oc} = 0.80 V, and *FF* = 58%) and RP3 (*PCE* = 2.21%, J_{sc} = 10.30 mA/cm^2, V_{oc} = 0.63 V, and *FF* = 34%) with those of their parent alternating polymer (repeating unit m) PBDTT-DPPD[32] (*PCE* = 6.57%, V_{oc} = 0.90 V, J_{sc} = 10.12 mA/cm^2, and *FF* = 72%) suggests that all three copolymers had a slightly improved photo-current, but the increase was not high. In addition, the V_{oc} and *FF* values were lowered significantly for all three copolymers, and consequently *PCEs* for three copolymers were lower than that for PBDTT-DPPD. On the other hand, a comparison of the photovoltaic parameters of

RP1, RP2 and RP3 with their corresponding low band gap alternating polymers (repeating unit n) such as PBDTT-TPD (*PCE* = 6.50%, J_{sc} = 11.10 mA/cm^2, V_{oc} = 1.00 V, and *FF* = 58%),[29] PBDTT-TT (*PCE* = 7.01%, J_{sc} = 14.10 mA/cm^2, V_{oc} = 0.78 V, and *FF* = 64%)[37] and PBDTT-DPP (*PCE* = 6.50%, J_{sc} = 13.70 mA/cm^2, V_{oc} = 0.73 V, and *FF* = 65%)[31] showed that all three copolymers offered relatively lower photovoltaic parameters. However, all three copolymers offered comparable V_{oc} (0.9 V, 0.8 V and 0.7 V, respectively) and *FF* values (67%, 58% and 47%, respectively) for the PSCs made from lower concentrations of copolymer:PC$_{70}$BM blend solutions, but the dramatically decreased J_{sc} led to a relatively lower *PCE* compared to that of its corresponding low band gap alternating polymers. Interestingly, RP1 and RP2 showed quite similar device performance but RP3 displayed poor performance compared to that of their corresponding alternating polymers.

This study strongly suggests that the incorporation of a strong electron deficient unit containing electron accepting functional groups as side groups (for example, TPD or TT units) on the PBDTT-DPPD backbone offered low band gap random copolymers showing a broad absorption band, high hole mobility and comparable *PCE* with that of PBDTT-DPPD. In contrast, the incorporation of a strong electron deficient unit containing electron accepting functional groups on its main part (for example, DPP) on the PBDTT-DPPD backbone gave low band gap random copolymers showing a broad absorption band, lower hole mobility and poor *PCE* compared to that of PBDTT-DPPD. These results are expected to provide useful information in designing new highly efficient random copolymers for PSCs.

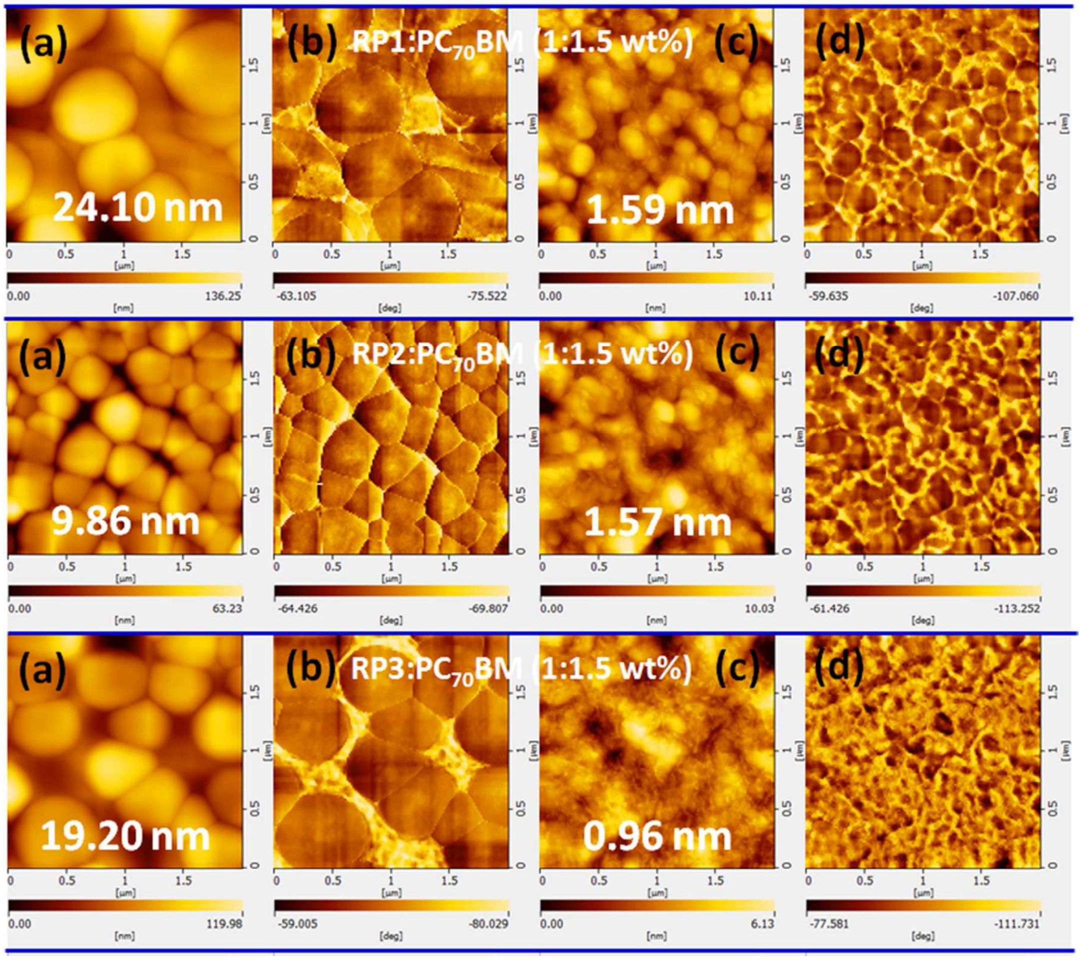

Fig. 9 Tapping (a and c) and phase (b and d) mode AFM images of the films made from polymer:PC$_{70}$BM blends without (a and b) and with 3 vol% DIO (c and d).

4. Conclusions

The optical, electrochemical, charge transport and photovoltaic properties of the highly efficient large band gap alternating polymer (PBDTT-DPPD) containing electron rich benzodithiophene (BDTT) and a weak electron deficient pyrrolo[3,4-c]pyrrole-1,3-dione (DPPD) derivatives were tuned by the insertion of a relatively strong electron deficient unit, such as thieno[3,4-c]pyrrole-4,6-dione (TPD), thieno[3,4-b]thiophene (TT) or pyrrolo[3,4-c]pyrrole-1,4-dione (DPP) derivative, on its backbone. The random copolymers containing two different electron acceptor units showed a broader absorption band than that of PBDTT-DPPD, and the band gap decreased with increasing the electron accepting ability of the strong electron acceptor units. The HOMO energy levels of random copolymers were similar or slightly higher, but the LUMO energy levels were significantly lower than that of PBDTT-DPPD. The random copolymers incorporating a strong electron deficient unit containing electron acceptor groups as side groups gave higher hole mobility. On the other hand, the random copolymer incorporating a strong electron deficient unit containing electron acceptor groups on its backbone gave lower hole mobility than that of PBDTT-DPPD. Random copolymers showed a comparable V_{oc} and *FF*, but the lower J_{sc} decreases their overall photovoltaic performances compared to those of their parent alternating polymers. The PSCs device optimization might improve the device performances. In this study, we demonstrated that broad absorbing and low band gap polymers that show high mobility and reasonable photovoltaic performances could be prepared by the incorporation of suitable weak and strong electron donor units in the polymer backbone. This study will be very useful for designing new materials for PSCs.

Acknowledgements

This research was supported by the National Research Foundation of Korea (NRF-2013R1A2A2A04014576). S. C. acknowledges the support by the Priority Research Centers Program (2009-0093818) at the University of Ulsan.

Notes and references

1 R. Sondergaard, M. Hosel, D. Angmo, T. T. Larsen-Olsen and F. C. Krebs, *Mater. Today,* 2012, **15**, 36.
2 A. C. Mayer, S. R. Scully, B. E. Hardin, M. W. Rowell and M. D. McGehee, *Mater. Today,* 2007, **10**, 28.
3 Y. Liu, J. Zhao1, Z. Li, C. Mu, W. Ma, H. Hu, K. Jiang, H. Lin, H. Ade and H. Yan, *Nat. Commun.,* 2014, **5**, 5293.
4 J.-D. Chen, C. Cui, Y.-Q. Li, L. Zhou, Q.-D. Ou, C. Li, Y. Li and J.-X. Tang, *Adv. Mater.,* 2014, **27**, 1035.
5 X. Guo, A. Facchetti and T. J. Marks, *Chem. Rev.,* 2014, **114**, 8943.
6 A. Pron and M. Leclerc, *Prog. Polym. Sci.,* 2013, **38**, 1815.
7 L. Huo and J. Hou, *Polym. Chem.,* 2011, **2**, 2453.
8 C. Gao, L. Wang, X. Li and H. Wang, *Polym. Chem.,* 2014, **5**, 5200.
9 Y.-Y. Lai, Y.-J. Cheng and C.-S. Hsu, *Energy Environ. Sci.,* 2014, **7**, 1866.
10 D. Mi, J.-H. Kim, H. U. Kim, F. Xu and D.-H. Hwang, *J. Nanosci. Nanotechnol.*, 2014, **14**, 1064.
11 P. Hudhomme, *EPJ Photovolt.,* 2013, **4**, 40401.
12 H.-C. Liao, C.-C. Ho, C.-Y. Chang, M.-H. Jao, S. B. Darling and W.-F. Su, *Mater. Today.,* 2013, **16**, 326.
13 B. R. Aich, J. Lu, S. Beaupre, M. Leclerc and Y. Tao, *Org. Electron.*, 2012, **13**, 1736.
14 C.-C. Chen, W.-H. Chang, K. Yoshimura, K. Ohya, J. You, J. Gao, Z. Hong and Y. Yang, *Adv. Mater.,* 2014, **26**, 5670.
15 J. Youa, L. Doua, Z. Hongc, G. Li and Y. Yang, *Prog. Polym. Sci.,* 2013, **38**, 1909.
16 W. Li, A. Furlan, K. H. Hendriks, M. M. Wienk and R. A. J. Janssen, *J. Am. Chem. Soc.,* 2013, **135**, 5529.
17 K. Li, Z. Li, K. Feng, X. Xu, L. Wang and Q. Peng, *J. Am. Chem. Soc.,* 2013, **135**, 13549.
18 J. You, L. Dou, K. Yoshimura, T. Kato, K. Ohya, T. Moriarty, K. Emery, C.-C. Chen, J. Gao, G. Li and Y. Yang, *Nat. Commun.,* 2013, **4**, 1446.
19 L. Dou, J. You, J. Yang, C.-C. Chen, Y. He, S. Murase, T. Moriarty, K. Emery, G. Li and Y. Yang, *Nat. Photonics,* 2012, **6**, 180.
20 Z. He, B. Xiao, F. Liu, H. Wu, Y. Yang, S. Xiao, C. Wang, T. P. Russell and Y. Cao, *Nat. Photonics,* 2015, **9**, 174.
21 W.-H. Chang, L. Meng, L. Dou, J. You, C.-C. Chen, Y. Yang, E. P. Young, G. Li and Y. Yang, *Macromolecules,* 2015, **48**, 562.
22 S.-H. Liao , H.-J. Jhuo , Y.-S. Cheng and S.-A. Chen, *Adv. Mater.,* 2013, **25**, 4766.
23 L. Lu, T. Xu, W. Chen, E. S. Landry and L. Yu, *Nat. Photonics,* 2014, **8**, 716.
24 T. Ameri, P. Khoram, J. Min and C. J. Brabec, *Adv. Mater.,* 2013, **25**, 4245.
25 A. C. Stuart, J. R. Tumbleston, H. Zhou, W. Li, S. Liu, H. Ade and W. You, *J. Am. Chem. Soc.,* 2013, **135**, 1806.
26 N. Wang, Z. Chen, W. Wei and Z. Jiang, *J. Am. Chem. Soc.,* 2013, **135**, 17060.
27 H. Zhou, L. Yang, A. C. Stuart, S. C. Price, S. Liu and W. You, *Angew. Chem., Int. Ed.,* 2011, **50**, 2995.
28 J.-H. Kim, J. B. Park, F. Xu, D. Kim, J. Kwak, A. C. Grimsdale and D.-H. Hwang, *Energy Environ. Sci.,* 2014, **7**, 4118.
29 J. Warnan, A. E. Labban, C. Cabanetos, E. T. Hoke, P. K. Shukla, C. Risko, J.-L. Bredas, M. D. McGehee and P. M. Beaujuge, *Chem. Mater.,* 2014, **26**, 2299.
30 L. Dou, J. Gao, E. Richard, J. You, C.-C. Chen, K. C. Cha, Y. He, G. Li and Y. Yang, *J. Am. Chem. Soc.,* 2012, **134**, 10071.
31 L. Dou, W.-H. Chang, J. Gao, C.-C. Chen, J. You and Y. Yang, *Adv. Mater.,* 2013, **25**, 825.
32 V. Tamilavan, K. H. Roh, R. Agneeswari, D. Y. Lee, S. Cho, Y. Jin, S. H. Park and M. H. Hyun, *J. Polym. Sci. A Polym. Chem.,* 2014, **52**, 3564.
33 V. Tamilavan, K. H. Roh, R. Agneeswari, D. Y. Lee, S. Cho, Y. Jin, S. H. Park and M. H. Hyun, *J. Mater. Chem. A,* 2014, **2**, 20126.
34 V. Tamilavan, J. Lee, R. Agneeswari, D. Y. Lee, S. Cho, Y. Jin, S. H. Park and M. H. Hyun, *Polymer,* 2015, **65**, 243.
35 V. Tamilavan, M. Song, R. Agneeswari, J.-W. Kang, D.-H. Hwang and M. H. Hyun, *Polymer,* 2013, **54**, 6125.
36 C. Guo , B. Sun and Y. Li , *Polym. Chem.,* 2014, **5**, 5247 .
37 L. Zhao, S. Zhao, Z. Xu, Q. Yang, D. Huanga and X. Xu, *Nanoscale,* 2015, **7**, 5537.

Properties modulation of pyrrolo[3,4-c]pyrrole-1,3-dione (DPPD)-based high energy converting large band gap polymer (PBDTT-DPPD) was studied via the incorporation of strong electron accepting thieno[3,4-c]pyrrole-4,6-dione (TPD), thieno[3,4-b]thiophene (TT) or pyrrolo[3,4-c]pyrrole-1,4-dione (DPP) unit on the polymer backbone.